Supplementary Information

Classification of prostate cancer using a protease activity nanosensor library

Authors: Jaideep S. Dudani[1,2], Maria Ibrahim[1,3], Jesse Kirkpatrick[1,3], Andrew D. Warren[1,3,8], Sangeeta N. Bhatia[1,3-7,*]

Affiliations:

1. Koch Institute for Integrative Cancer Research, Massachusetts Institute of Technology, Cambridge, MA 02139
2. Department of Biological Engineering, Massachusetts Institute of Technology, Cambridge, MA 02139
3. Harvard–MIT Division of Health Sciences and Technology, Institute for Medical Engineering and Science, Massachusetts Institute of Technology, Cambridge, MA 02139
4. Department of Electrical Engineering and Computer Science, Massachusetts Institute of Technology, Cambridge, MA 02139
5. Department of Medicine, Brigham and Women's Hospital and Harvard Medical School, Boston, MA 02115
6. Broad Institute of Massachusetts Institute of Technology and Harvard, Cambridge, MA 02139
7. Howard Hughes Medical Institute, Cambridge, MA 02139

*Corresponding Author: Sangeeta N. Bhatia
Address: 500 Main Street, 76-453, Cambridge, MA 02142, USA
Phone: 617-253-0893
Fax: 617-324-0740
Email: sbhatia@mit.edu

www.pnas.org/cgi/doi/10.1073/pnas.1805337115

Supplementary Methods

Peptide synthesis and conjugations. Peptides used in this study were either synthesized by CPC Scientific, Inc or Tufts Peptide Core. For FRET assays, peptides were flanked by fluorophore-quencher pairs; for urine experiments, peptides were either barcoded with a Biotin and a fluorophore or heavy isotopes for mass spectrometry.

A D-stereoisomer of glutamate fibrinopeptide, either flanked by a Biotin/ligand for ELISA and imaging or heavy isotope encoded, was used as the urinary reporter. Multivalent PEG (40 kDa, eight-arm) containing maleimide reactive handles (JenKem Technology) was dissolved in PBS and filtered (pore size: 0.2 μm). After filtration, the cysteine-terminated peptides were added at 20-fold excess to the PEG and reacted for at least 1 hour. Unconjugated peptide was filtered using fast-protein liquid chromatography (FPLC, GE Healthcare) or by spin filters (MWCO = 10 kDa, Millipore). Concentration was quantified by extinction coefficients of ligands. Particles were stored at 4 °C in PBS.

Mass-encoded reporters were designed based on our iCORE scheme. Conjugation of mass-encoded peptides to PEG was performed at CPC Scientific, Inc and lyophilized. Lyophilized PEGylated peptides were dissolved in mannitol/sodium phosphate buffer at 1 mg/mL and pooled into the final library.

We expect given the excess of peptides to PEG in the conjugation reaction that we are coupling 8 peptides per PEG. Indeed, we see a single species in most of our analysis by RP-HPLC (see Table S4). For in vivo experiments with MS readouts, each peptide was injected at 5 μM in 200 μL per mouse, and for experiments with the 3-plex particles, each particle was injected at 1 μM in 200 μL per mouse.

Transcriptomic analysis. RNA-Seq data were generated by the TCGA Research Network (http://cancergenome.nih.gov). The list of human extracellular endoprotease genes was obtained from UniProt. Clinical characteristics associated with each sample was downloaded from FireBrowse (http://firebrowse.org). Differential expression analysis was performed using SAMseq. All median fold-changes of 1.5 or greater were kept in the initial analysis. For filtering, tissue expression was analyzed on a case-by-case basis using the GTex Portal (https://www.gtexportal.org/home/), as was identification of recombinant versions of proteases and potential substrates.

For SOMAscan, fresh frozen prostate cancer and matched normal adjacent samples were acquired from DxBio. The data was normalized for plate hybridization and analyzed for protein fold changes. HPN, KLK2, MMP26, and MMP11 are not part of the assay.

Recombinant protease substrate screening. Screens were performed in a 384 well plate in duplicate in enzyme-specific buffer with peptides (1 μM) and proteases (12.5 nM) in 30 μL at 37 °C. Fluorescence was measured using a Tecan plate reader. Signal increase at 30 minutes was used across conditions. Buffer conditions were: MMPs (50mM TRIS, pH 7.5, 10 mM $CaCl_2$, 300 mM NaCl, 20 μM $ZnCl_2$, 0.02% Brij-35, 1% BSA), ADAM12 (20 mM Tris, pH 8.0, 6e-4 Brij-35, 1% BSA), KLKs/PRSS3 (50 mM Tris, 0.15 M NaCl, 10 mM $CaCl_2$, 0.05% Brij-35, pH 7.5, 1% BSA), uPA (50 mM Tris, 0.01% Tween 20, pH 7.4, 1% BSA), Hepsin (100mM Tris, pH 9.0, 1% BSA), and Thrombin/Factor Xa (PBS, 1% BSA). Peptides were plated out in 384 well plates using a plate spotter at the KI High-Throughput Screening Core.

Cell culture experiments. Cell lines were purchased from the American Type Culture Collection (ATCC) and cultured according to supplier protocols. The Matrigel invasion assay was carried out according to the manufacturer's instructions (BioCoat Matrigel Invasion Chambers, Corning). For supernatant cleavage assays, cells were cultured in Optimem

overnight in 6 well plates and supernatant was collected. Protein was quantified and normalized across samples.

For matrigel assays, cells were fixed in 100% methanol, stained with Wright-Giemsa, and counted under a microscope. Matrigel invasion for each experimental group was measured in triplicate. Protease Inhibitor Cocktail (P1860, Sigma) was diluted 1:500 in DMSO and added to the upper chamber. The control wells contained .5% total volume DMSO.

For supernatant cleavage assays, cells cultured in 22Rv1 or PC3 cells were seeded in a 6 well plate at a density of 5×10^4 in complete media for 24 hours. Media was replaced with Optimem for 24 hours. Supernatant was collected, centrifuged, and stored at -20 °C. Protein concentration was measured using BCA Protein Assay Kit and normalized across samples. Marimastat (Sigma) was used at a final concentration of 50 μM. AEBSF and E64 were dissolved in distilled water and used at a final concentration of 500 μM and 100 μM, respectively. The plates were incubated at 37°C.

Animal models. For PK studies, wildtype, male Swiss-Webster mice (4−6 weeks, Taconic) were infused intravenously with VT-750 (Perkin Elmer)-labeled nanoparticles. For prostate inflammation comparison, NOD mice (Jackson Lab) were injected intravenously with nanoparticle at 8 and 20 weeks and urine was collected.

After injection with nanoparticle, mice were placed into custom housing with a 96-well plate base for urine collection. The bladders were voided to collect between 100-200 uL of urine at 1 and 2 hours post injection. Urine was centrifuged and stored at -20°C. After xenograft implantation, tumors were measured with a digital caliper and volumes were calculated as volume $=0.5 \times \text{length} \times \text{width}^2$, where length and width are the larger and smaller dimensions, respectively. Total tumor volume was defined as the sum of the tumor volume in each flank.

For PSA ELISA, approximately 200 μL of blood was collected and spiked with EDTA to a final concentration of 5 mM and blood cells were pelleted. Plasma was stored at -20 ºC prior to PSA quantification. PSA levels were measured using the PSA quantikine ELISA kit according to manufacturer protocols (R&D Systems).

For NOD mice, prostates were harvested from mice in both age groups, H&E stained, and analyzed for inflammation by Dr. R.T. Bronson, a veterinary pathologist blinded to the tissue samples. For PK experiments, PEG (8-arm, 40 kDA; Jenkem), 10 and 20 nm dextran-coated iron oxide particles (Ocean Nanotech) were injected at equal concentration by fluorophore. Three hours post injection, organs were harvested and scanned on a Li-Cor for VT-750 signal.

Histology. Sectioning and staining was performed by the KI Histology Core. Organs were fixed in 10% formalin after necropsy and stored at 4 °C prior to embedding into paraffin, sectioning, and staining. PC3 and 22Rv1 tumor sections were stained for uPA (sc-14019; 1:100), MMP13 (ab84594; 1:200), αv integrin (Millipore AB1930; 1:200), and PEG (ab26A04; 1:175.) Prostate cancer TMA was obtained from US Biomax, Inc. (PR484) and stained for KLK14 (LS- C415470; 1:200), MMP26 (18087-1-AP; 1:100), and αv integrin. Staining intensity was quantified by Dr. R.T. Bronson.

Ex vivo activity assays. Tissue samples were homogenized at 100 mg/mL and centrifuged. Supernatant was placed into 384 well plate with FRET peptides and fluorescence signal increase was measured using a Tecan plate reader.

For tumor homogenates, supernatant was placed into 384 well plates with or without Marimastat at 50 μM.

Urine reporter analysis. Custom sandwich ELISAs were done as previously described (Warren et al, *PNAS* 2014), as was Cy7 imaging (Kwon et al, *Nature Biomedical Engineering* 2017). Mass-spectrometry analysis was performed at Inventiv Health in a process similar to our previous work (15).

Briefly, urine was collected and stored at -80 ºC. Photolysis of the photolabile group was performed under UV light to yield the reporter parent mass. LC-MS/MS was performed on the urine and the y6 ion was quantified. An internal control reporter was spiked into the urine prior to analysis. Data was normalized by this internal reporter and the injected free reporter and mean normalized for analysis.

Statistics. Analysis was either performed using MATLAB or GraphPad Prism. Details of each statistical test are included in figure legends.

Supplementary Figures and Tables

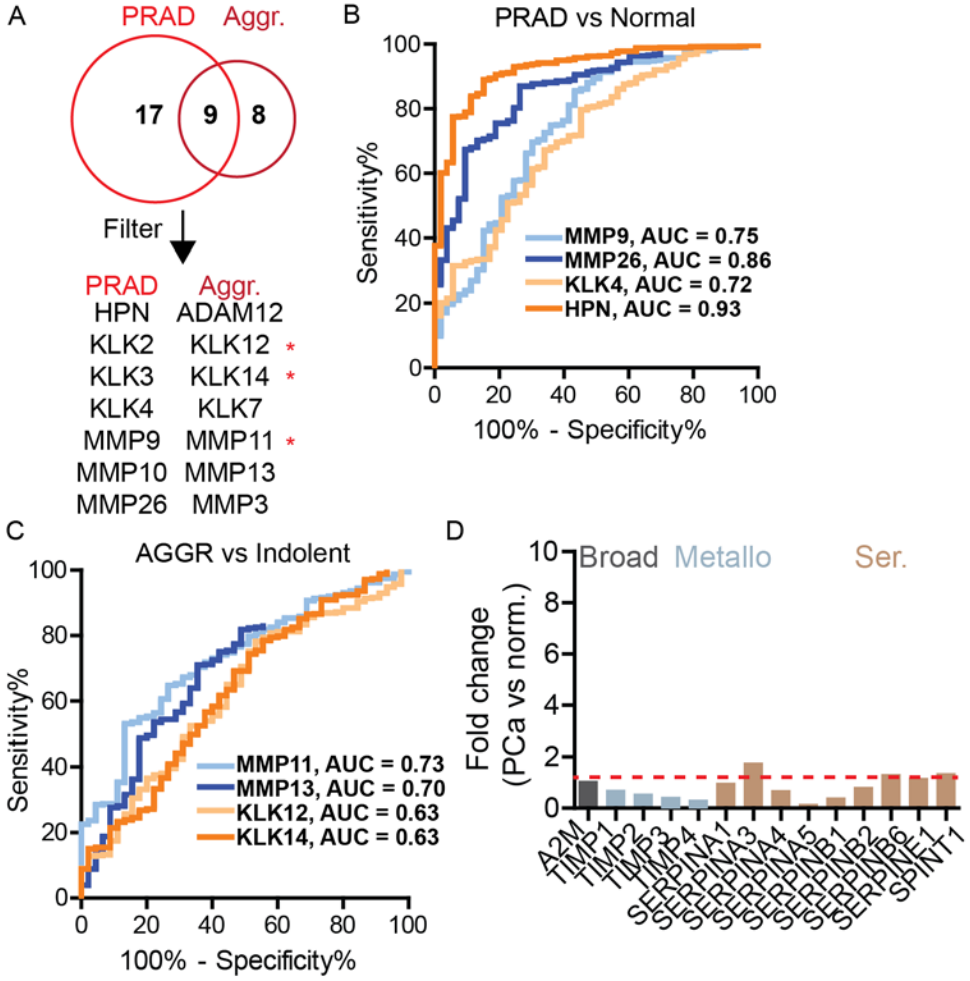

Figure S1. Protease and inhibitor expression analysis in TCGA. (A) Hit proteases were selected based on fold change > 1.5. A total of 34 proteases were identified, with 9 shared between two lists. These hits were filtered on criteria such as availability of recombinant protease, substrate specificity, and literature analysis to yield a final list of 14 between the two lists. This includes comparing transcript levels to healthy tissues using the GTex Portal. *: Shared between both lists. (B) Example proteases from the PRAD list demonstrating robust classification potential of cancer vs normal. (C) Example proteases from the AGGR list

demonstrating robust classification potential of aggressive (Gleason 7-10) vs Gleason 6. (D) Fold change of protease inhibitors in TCGA comparing cancer tissue expression vs normal adjacent tissue.

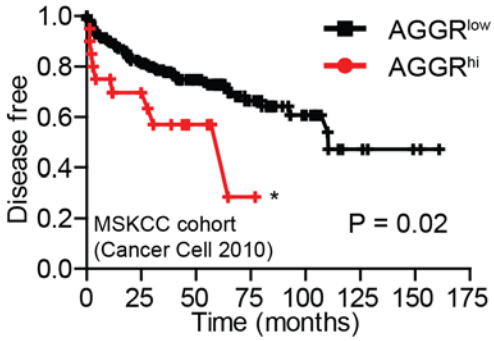

Figure S2. Disease-free survival stratification in the MSKCC cohort based on expression of proteases in the AGGR list.

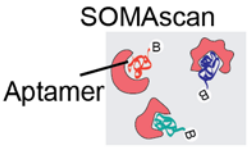

#	T	N	G	%T
1	T2c	N0	3+3	30
2			4+3	70
3	T3	N1	4+4	80
4	T3a	Nx	4+5	50
5	T3b	N0	4+5	70

Figure S3. Human patient sample characteristics and SOMAscan schematic. T and N reference the TNM staging system; G: Gleason, %T: percent tumor in sample.

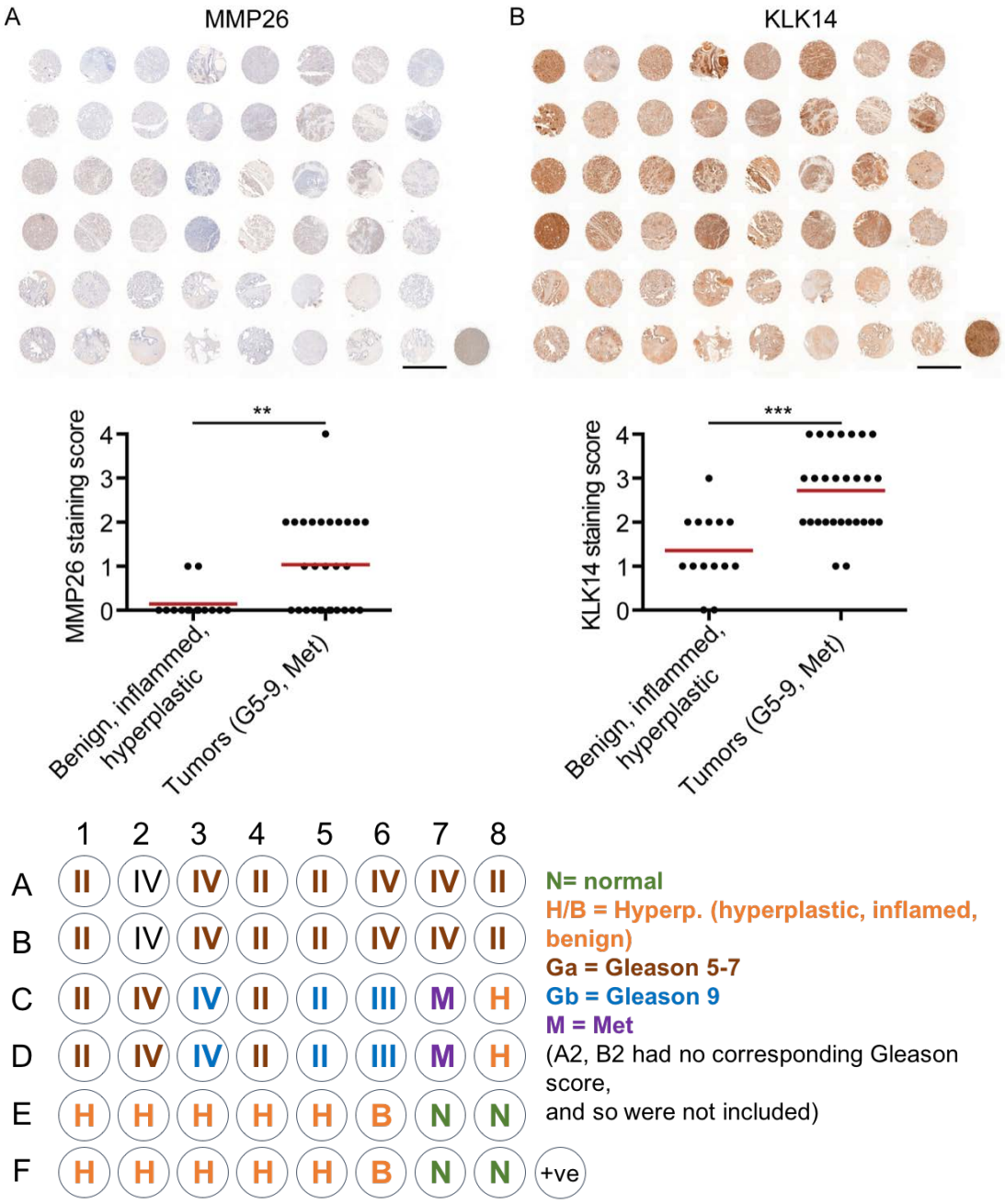

Figure S4. IHC staining of proteases in TMAs. (A) MMP26 IHC stain and comparison of staining intensity between tumor samples and potentially confounding conditions (hyperplasia, benign tumor, inflammation). (B) KLK14 IHC stain and comparison of staining intensity between tumor samples and potentially confounding conditions (hyperplasia, benign tumor, inflammation). A-B: Student's t test. Scale bar: 2 mm. Bottom: TMA map. Additional details can be found online at https://www.biomax.us/tissue-arrays/Prostate/PR484.

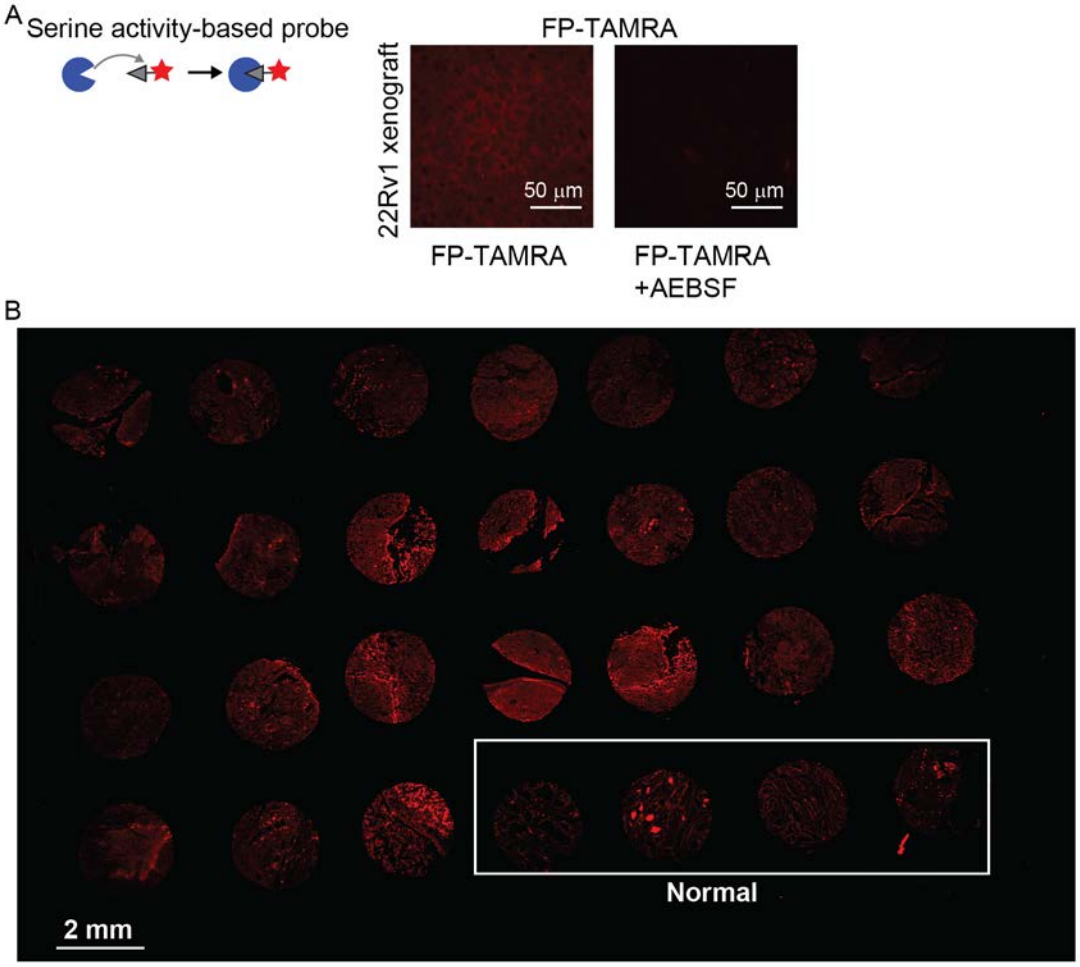

Figure S5. ABP analysis of serine hydrolase activity in prostate cancer. (A) Fresh frozen 22Rv1 sections were incubated with FP-TAMRA ABP and showed clear labeling that was inhibited by AEBSF. (B) Full prostate cancer TMA with ABP labeling.

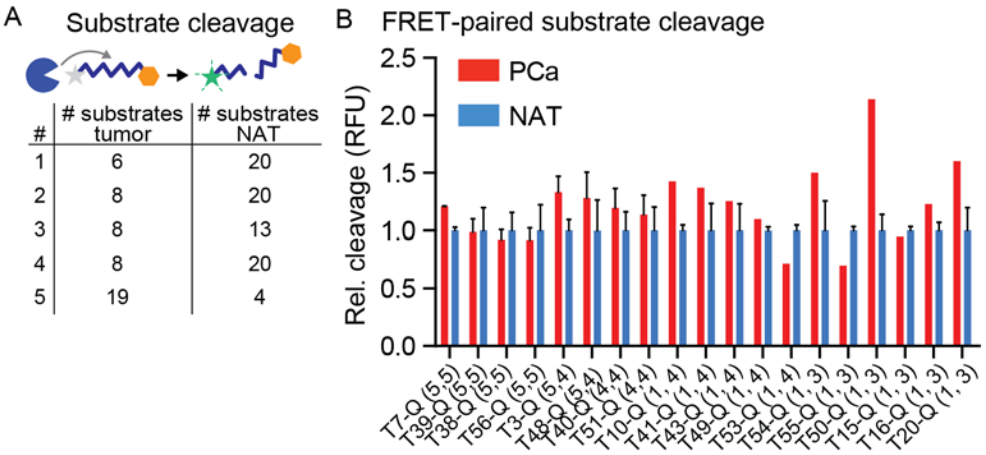

#	# substrates tumor	# substrates NAT
1	6	20
2	8	20
3	8	13
4	8	20
5	19	4

Figure S6. FRET substrate cleavage in human prostate cancer homogenates. (A) Human prostate cancer samples were homogenized and tested against FRET peptide substrates. Number of substrates evaluated against each sample. (B) Fluorescence signal from cleavage

across substrates was measured. Numbers in parentheses are the number of samples per substrate (first number: PCa, second number: NAT).

Table S1. Selected proteases for ABN development.

Protease	Catalytic type	List (PRAD / AGGR)	Transcript?	Protein?
ADAM12	Metallo	AGGR	Yes	Yes
HPN	Serine	PRAD	Yes	-
KLK2	Serine	PRAD	Yes	-
KLK3	Serine	PRAD	Yes	Yes
KLK4	Serine	PRAD	Yes	Yes
KLK12	Serine	Both	Yes	Yes
KLK14	Serine	Both	Yes	Yes
MMP3	Metallo	AGGR	Yes	Yes
MMP9	Metallo	PRAD	Yes	Yes
MMP10	Metallo	PRAD	Yes	Yes
MMP11	Metallo	Both	Yes	-
MMP13	Metallo	AGGR	Yes	Yes
MMP26	Metallo	PRAD	Yes	Yes
PRSS3	Serine	-	No	Yes
uPA	Serine	-	No	Yes

Table S2. Important peptides, nomenclature, and design.

Name	Sequence	Readout (sample type)
(T1-58)-Q	(5FAM)-(SUBSTRATE)-(CPQ2)-(PEG2)-C	Fluorescence (in vitro / ex vivo)
-M	(Heavy isotope D-Glu-Fib)-(ANP)-(SUBSTRATE)-C	Urine (LC-MS/MS)
T7-Q	(5FAM)-GGPLGVRGKK(CPQ2)-(PEG2)-C	Fluorescence (in vitro / ex vivo)
T7-QF	(QSY21)-GGPLGVRGKK(Cy5)-(PEG2)-C	Fluorescence (in vivo)
T7-B(DNP)	Biotin-eGvndneeGffsarK(DNP)GPLGVRGKGC	ELISA (urine)
T7-B(FAM)	Biotin-eGvndneeGffsarK(5FAM)GPLGVRGKGC	ELISA (urine)
T24-Q	(5FAM)-GGLGPKGQTGK(CPQ2)-(PEG2)-C	Fluorescence (in vitro / ex vivo)
T24-B(Cy7)	Biotin-eGvndneeGffsarK(Cy7)GGLGPKGQTGGC	Fluorescence (urine)
T39-Q	(5FAM)-GGGSGRSANAKG-K(CPQ2)-(PEG2)-GC	Fluorescence (in vitro / ex vivo)
T39-B(FAM)	Biotin-eGvndneeGffsarK(5FAM)GGGSGRSANAKGC	ELISA (urine)
ELISA reporter	Biotin-eGvndneeGffsarK(AF488)GGLGGGAGC	ELISA (urine)
iRGD	C–PEG2–CRGDKGPDC; Cys2&3 disulfide bridge	Tumor-penetrating peptide

Table S2 notes:

In most cases, peptide C terminus is $CONH_2$.

Lower case: D-stereoisomer.

Nomenclature: Q = quenched, B = biotin, M = mass-encoded.

For mass-encoding scheme, see **Fig. S12A**.

FAM-CPQ2: FRET pair, with FAM as fluorophore and CPQ2 as quencher.

Cy5-QSY21: Red-shifted FRET pair. Cy5: fluorophore, QSY21: quencher; order of fluorophore-quencher reversed in comparison to above.

5FAM, DNP, AF488 can be detected with an antibody; Cy7 measured by fluorescence.

ANP: 3-Amino-3-(2-nitrophenyl)propionic acid; photolabile group.

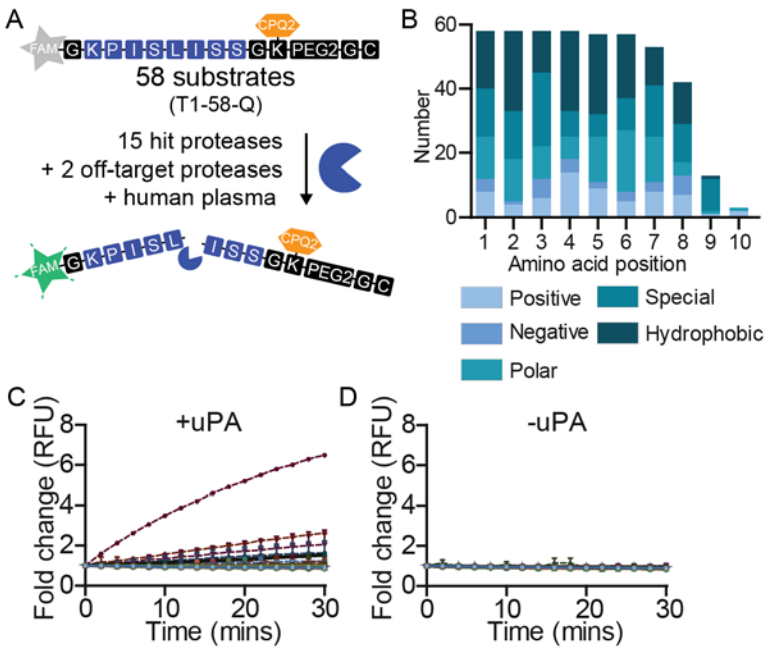

Figure S7. Recombinant protease cleavage of FRET peptides. (A) Recmombiant protease assay design. (B) Physiochemical properties of the substrate library. (C-D) Example fluorescent dequenching measurement for uPA. Each line is an individual substrate. In the absence of protease, no dequenching was observed. Assays were run in duplicate.

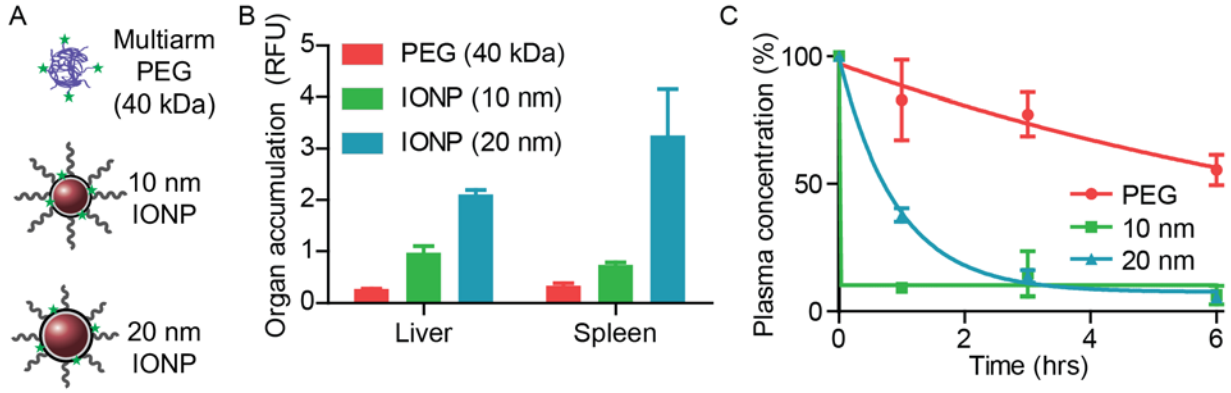

Figure S8. Pharmacokinetic analysis of nanocarriers. (A) Schematics of particles evaluated for prostate accumulation. (B) Liver and spleen accumulation of nanoparticles. (C) Plasma half-life shows rapid clearance of iron oxide particles, but long half-life of PEG, suggesting the ability to avoid the mononuclear phagocytic system.

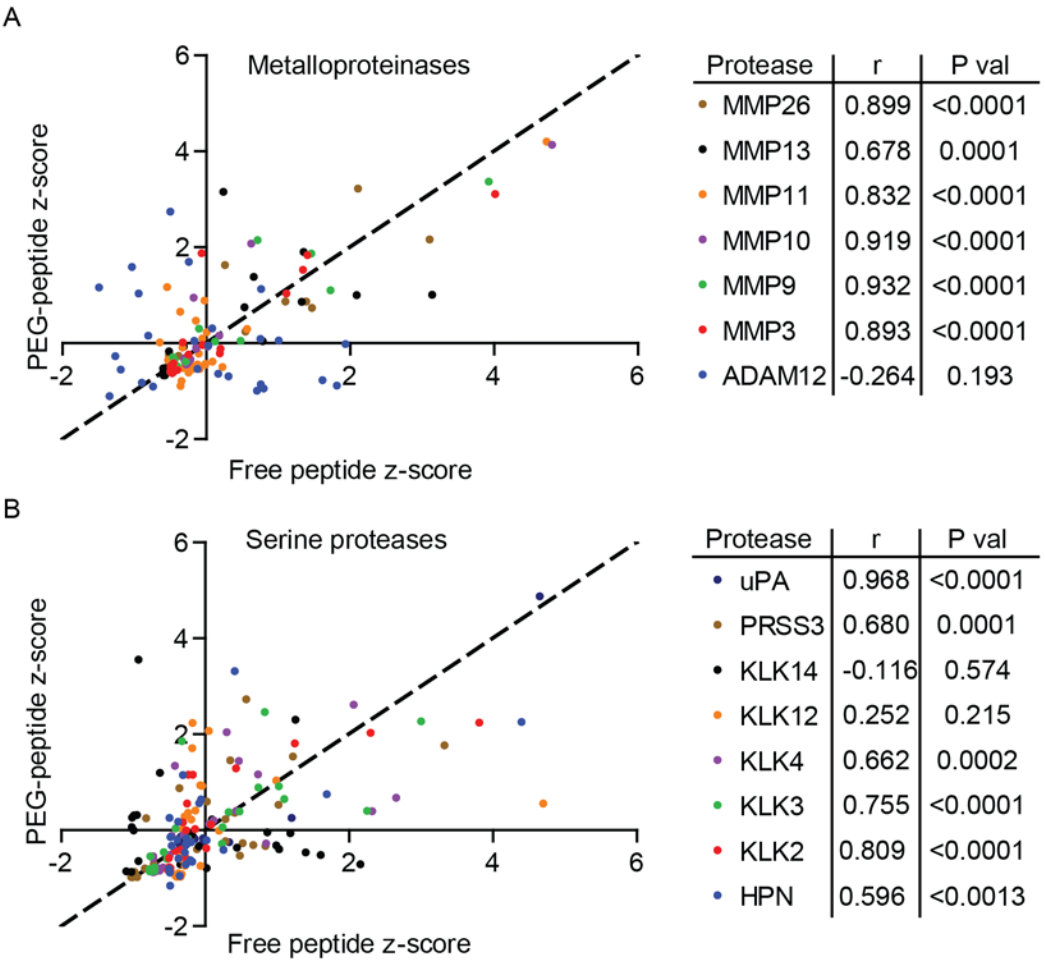

Figure S9. PEG-peptide conjugates screened against recombinant proteases. (A-B) Correlation of free peptide cleavage to PEG-peptide conjugate.

Table S3. Descriptive characteristics of ABN library.

Name	Top hit	Second hit	Additional notes
PEG-T1-Q	MMP9	-	HP
PEG-T2-Q	KLK2	KLK3	Thrombin
PEG-T3-Q	MMP9	-	-
PEG-T7-Q	MMP9	MMP26	-
PEG-T20-Q	KLKs	-	-
PEG-T24-Q	MMP13	-	-
PEG-T38-Q	KLK2	-	FXa
PEG-T39-Q	uPA	-	-
PEG-T40-Q	MMP26	ADAM12	-
PEG-T41-Q	ADAM12	-	Poorly cleaved
PEG-T43-Q	MMP3	-	-
PEG-T48-Q	HPN	KLK2	-

PEG-T49-Q	KLK14	PRSS3	-
PEG-T50-Q	KLK14	KLK12	-
PEG-T51-Q	KLK4	KLK3	-
PEG-T53-Q	MMP11	MMP26	Several MPs
PEG-T54-Q	ADAM12	MMP13	-
PEG-T56-Q	MMP10	MMP3	-
PEG-T58-Q	HPN	PRSS3	Several SPs

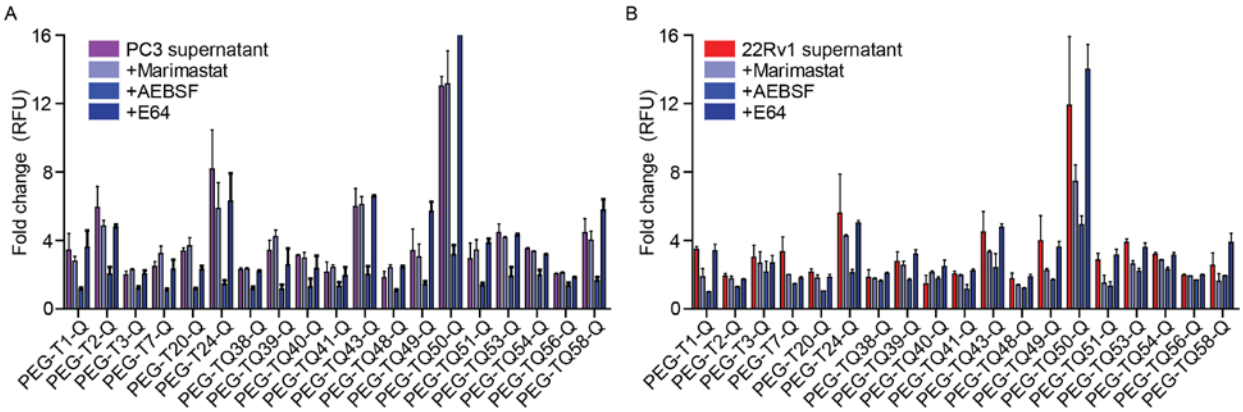

Figure S10. Cell-secreted proteases in supernatant cleave ABNs. Substrate cleavage of fluorogenic ABN library in the presence of (A) PC3 supernatant and (B) 22Rv1 supernatant with or without inhibitors.

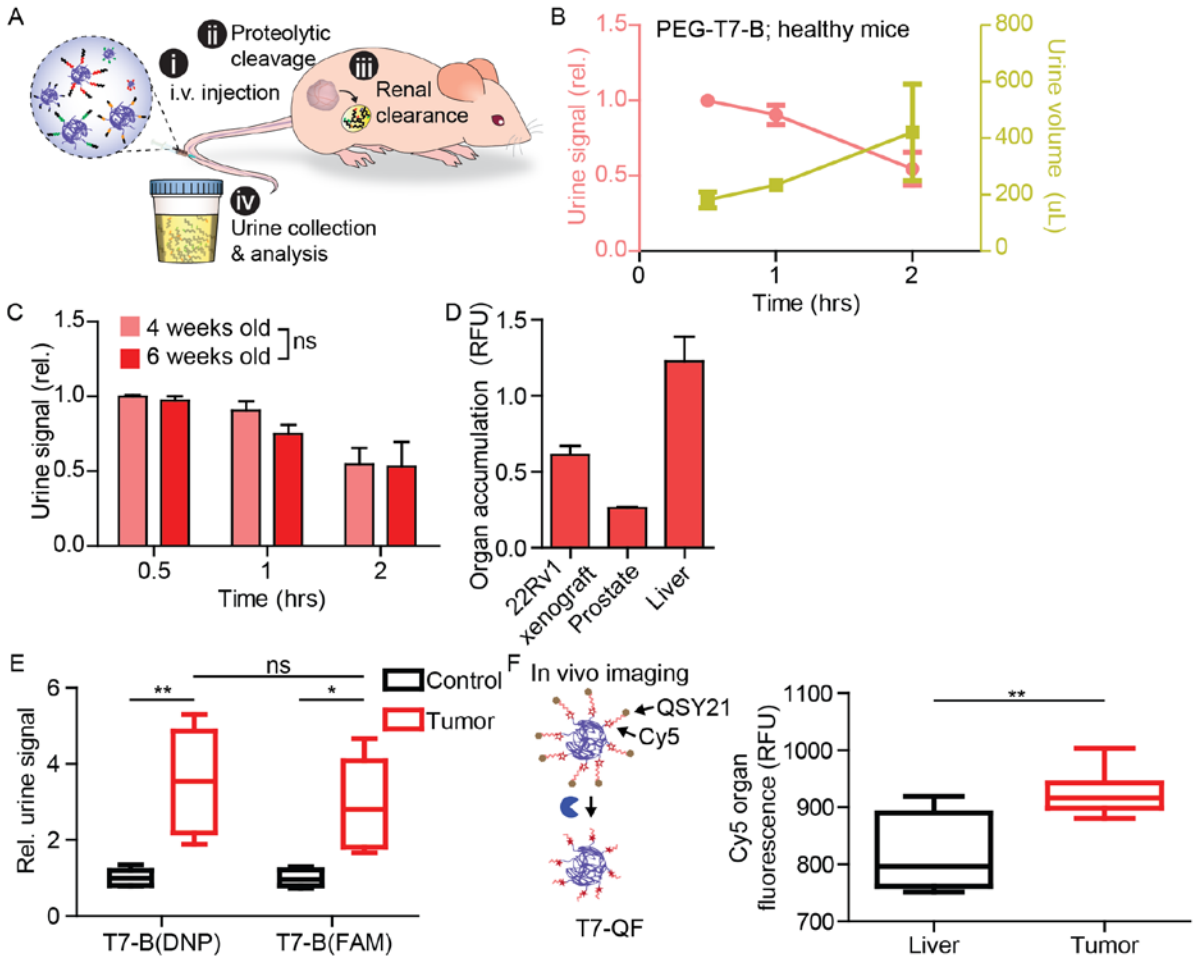

Figure S11. Evaluation of ABNs in vivo. (A) Design of in vivo ABN experiment. PEG-T7-B was initially used for optimization. (B) Urine signal and volume after injection of PEG-T7-B in healthy Swiss-Webster mice. (C) Urine signal is unchanged after a second injection two weeks later in healthy mice. (D) Fluorescently-labeled PEG significantly accumulated in flank 22Rv1 xenografts but to a lower extent than the liver. (E) The barcode does not impact ABN performance in 22Rv1-bearing mice. (F) In vivo imaging experiment with Cy5 quenched PEG-T7-QF shows greater 22Rv1 tumor signal compared to liver. (B-C: 2Way ANOVA, Tukey's multiple comparison test; D: Student's t test).

Table S4. Multiplexed ABNs with mass-encoded barcodes.

Substrate	Reporter	Reporter parent mass	y6 transition quantifier	Peptide MW	PEG-peptide MW	PEG-peptide purity
T40	R3_01	789.3	683.8	2813	62504	90.4%
T2	R3_02	789.3	685.8	2710.9	61687.2	94.0%
T3	R3_03	789.3	687.8	2580.8	60646.4	95.6%
T7	R3_04	789.3	689.8	2752	62016	92.4%
T20	R3_05	789.3	691.8	2914.1	63312.8	94.0%
T24	R3_06	792.3	689.8	2788.9	62311.2	94.9%
T38	R3_08	792.3	693.8	3031.3	64250.4	43.6%

T39	R3_09	792.3	695.8	2879	63032	93.7%
T41	R3_10	792.3	697.8	2789	62312	93.3%
T1	R3_11	795.3	695.8	2822.9	62583.2	95.8%
T43	R3_12	795.3	697.8	3275.6	66204.8	94.1%
T48	R3_13	795.3	699.8	2839	62712	94.3%
T49	R3_14	795.3	701.8	2465.6	59724.8	90.2%
T50	R3_15	795.3	703.8	2698.8	61590.4	90.7%
T51	R3_16	798.3	701.8	2631.7	61053.6	92.0%
T53	R3_17	798.3	703.8	2792.9	62343.2	96.0%
T54	R3_18	798.3	705.8	3002	64017.6	62.1%
T56	R3_19	798.3	707.8	2842.1	62736.8	92.0%
T58	R3_20	798.3	709.8	2799.9	62399.2	96.2%
Reporter	R3_00	803.3	710.77	803.3	-	-

Table S4 notes:
This new generation of reporters enables increased multiplexing with improved readouts by using five barcodes per parent mass, with parent masses spaced by 3 Da and y6 ions spaced by 2 Da. PEG-peptide conjugations were analyzed by reverse-phase HPLC and determined to be greater than 90% for most particles. A few had lower calculated purity due to polydisperse populations but still were conjugated to PEG.

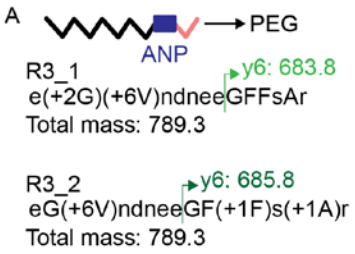

B

Reporter	R^2 (0-1000 ng/mL)
R3_01	0.992756
R3_02	0.994406
R3_03	0.993364
R3_04	0.994402
R3_05	0.994446
R3_06	0.99665
R3_07	0.992645
R3_08	0.994309
R3_09	0.993971
R3_10	0.995628
R3_11	0.992483
R3_12	0.995284
R3_13	0.990885
R3_14	0.994404
R3_15	0.994768
R3_16	0.992862
R3_17	0.994385
R3_18	0.994226
R3_19	0.996726
R3_20	0.993071
R3_00	0.997686

Figure S12. Mass-encoded ABN library performance. (A) Design of mass-encoded reporters showing reporter and photolabile group. (B) Analytical performance of each reporter shows large dynamic range, with robust linear fit from 0 to 1000 ng/mL in urine.

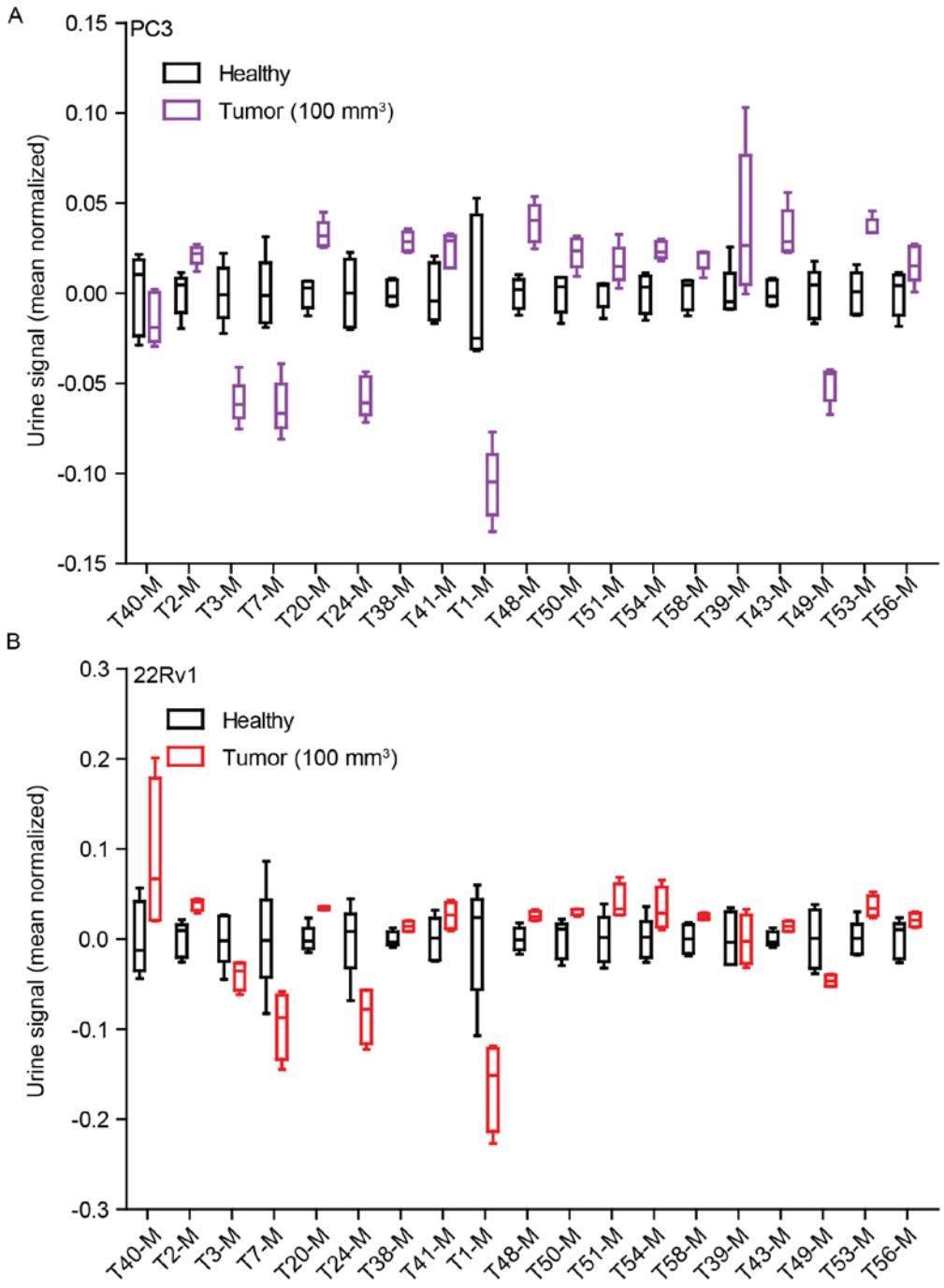

Figure S13. Urine signals from mass-encoded library. (A) Signal from PC3-bearing mice compared to healthy mice and (B) signal from 22Rv1-bearing mice compared to healthy. Data is mean-normalized and then signal change is plotted. Several signals move together for both PC3 and 22Rv1, but several change to a different magnitude or sign, such as T40 and T51 up in 22Rv1 and T24 and T39 up in PC3.

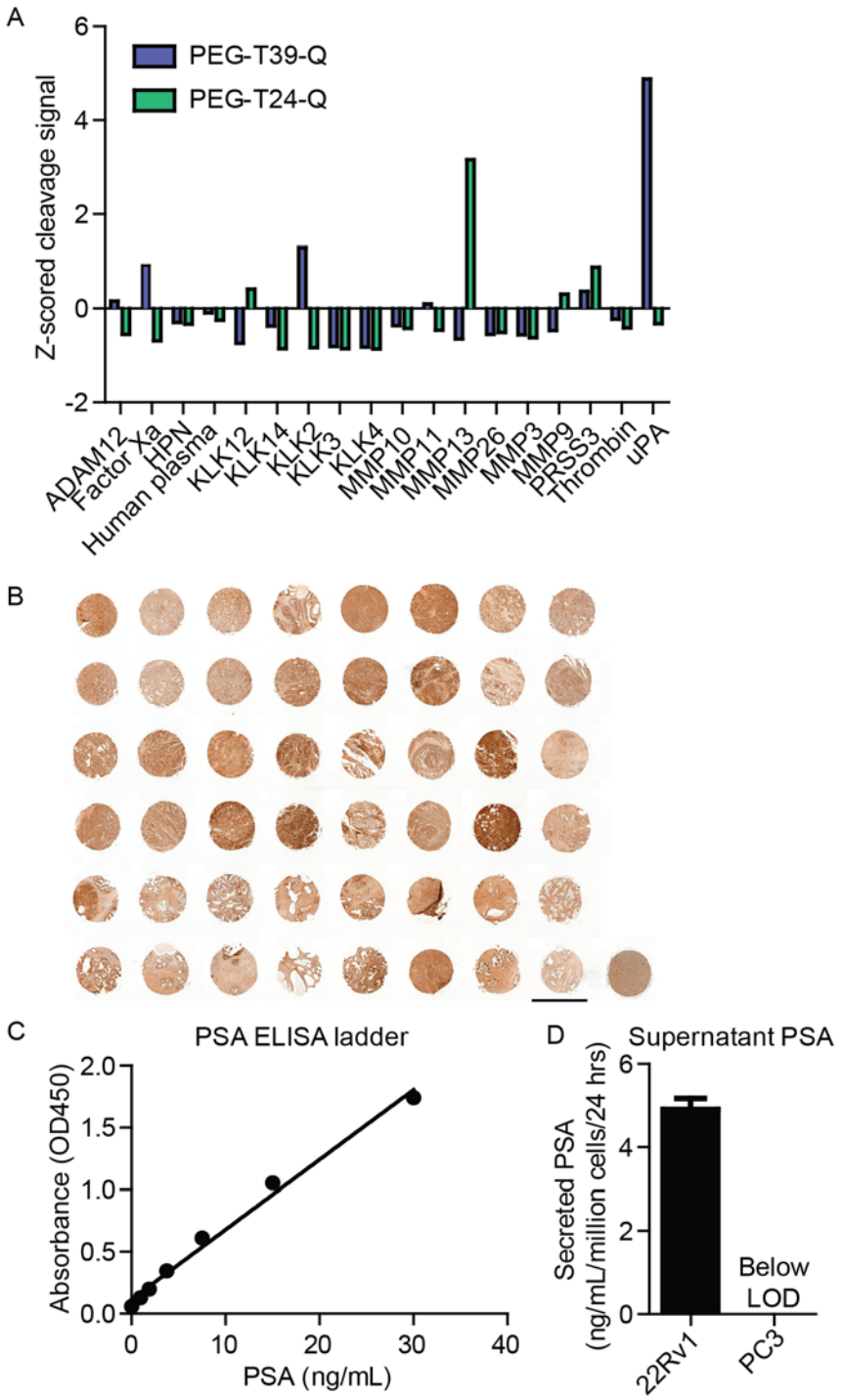

Figure S14. Characterization for integrin-targeted ABN subset. (A) Cleavage specificity for PEG-T39-Q and PEG-T24-Q by recombinant uPA and MMP13, respectively. (B) Full human prostate cancer TMA stained for α_v integrin. Scale bar: 2 mm. (C) PSA ELISA ladder. (D) PSA secretion rate from 22Rv1 cells and PC3 cells.

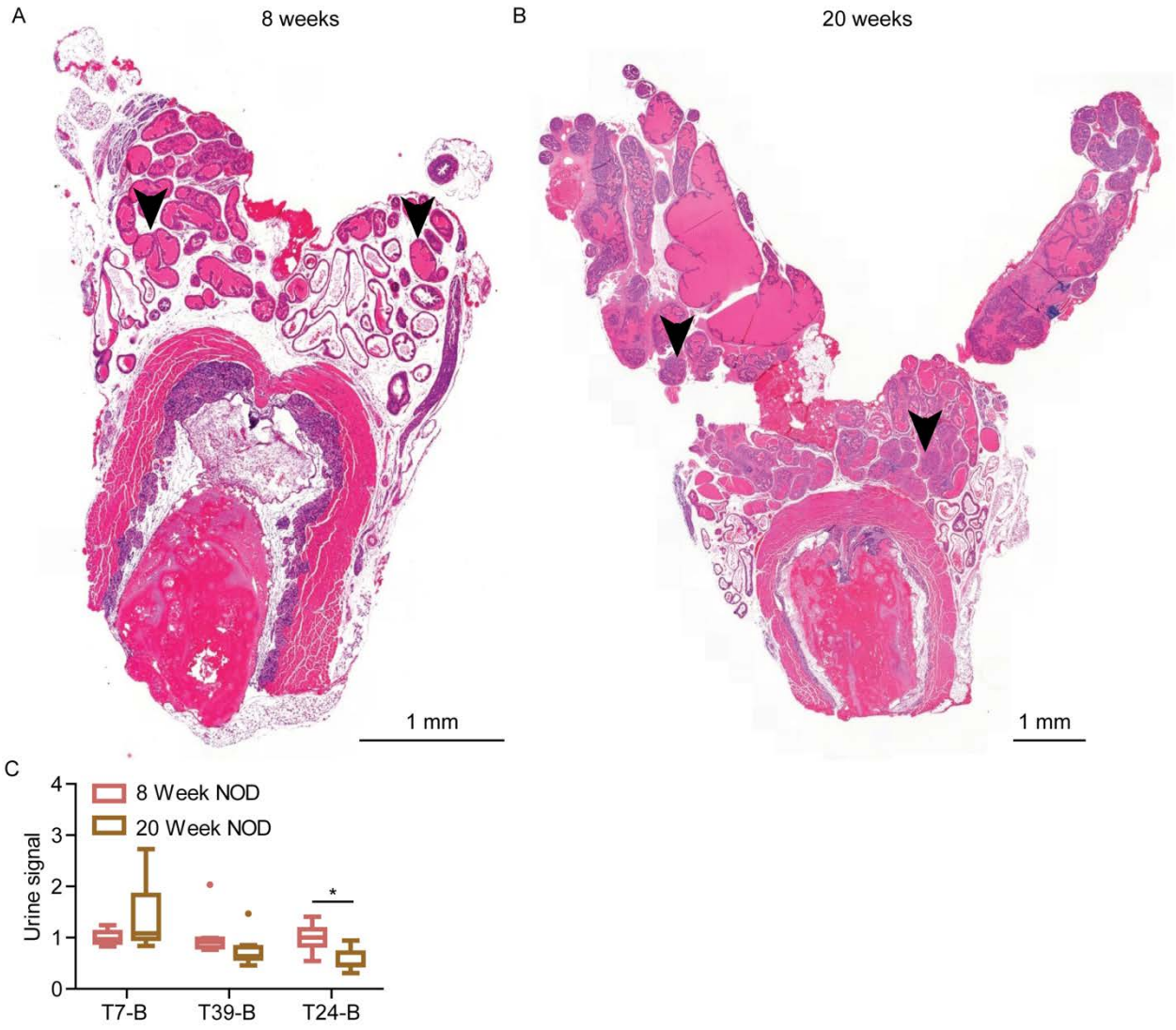

Figure S15. Evaluation of 3-plex iRGD ABNs in NOD mice. (A-B) Prostate enlargement and immune cell infiltration was noted in the older mice. Note difference in scale bar size. Prostate inflammation was confirmed by a veterinary pathologist. Arrows provide guides to contrast the infiltration in the prostate section from the older mouse. (C) Urine signal across substrates shows no increase in reporter concentration in older mice. (2Way ANOVA, Tukey's multiple comparison test).